Fiber Noise Cancellation for a 698 nm Laser in ^{88}Sr Quantum Experiments

Milan Boers | Third-year Applied Physics student at Amsterdam University of Applied Sciences | Internship Project | Student Number: 500928737



UNIVERSITY OF AMSTERDAM



Amsterdam University of Applied Sciences

NOVEMBER 25 2025

UoA SrMic Group | UoA Supervisor: Alex Urech | AUAS Supervisor: Moos van Caspel

Abstract

In this project, a fiber noise cancellation (FNC) system was developed and characterized to suppress the phase and frequency noise of a 698 nm laser used in the SrMic lab at the University of Amsterdam. This laser drives the ultra-narrow $^{1}S_{0} \rightarrow {}^{3}P_{0}$ transition in ^{88}Sr, which is crucial for quantum computing and quantum simulation experiments. Relatively long optical fibers give rise to substantial phase and frequency noise, decoherence, population loss in the desired quantum state, and increased errors during quantum operations.

To reduce this noise, an acousto-optic modulator (AOM)-based feedback loop was implemented, driven by a Direct Digital Synthesizer (DDS) inside an AOM-driver. The fiber-induced noise was measured using an analog mixer and a spectrum analyzer, after which both digital and analog PID controllers were tested to determine the optimal stabilization method.

The results show that the FNC system is most effective at low Fourier frequencies (0–5 kHz), where the RMS frequency noise is reduced from ~1262 Hz to ~25 Hz. This improvement is significant, as noise in this frequency band has the strongest impact on coherence and laser–atom interaction accuracy in this case.

These findings demonstrate that the developed FNC system is suitable for experiments where ^{88}Sr atoms are used for quantum computing/simulations and plays an important role in reducing errors and improving the stability of the 698 nm laser.

Table of Contents

1. Introduction 3
   1.1. Background 3
   1.2. Theory 4
      1.2.1. Fiber Noise 4
      1.2.2. Beat-note 4
      1.2.3. Power Spectral Density (PSD), Phase Noise & RBW / ENBW 4
      1.2.4. Frequency noise & RMS 5
      1.2.5. Acousto Optical Modulator (AOM), Polarizing Beam Splitter (PBS) & Faraday Isolator (FI) 6
      1.2.6. Red Pitaya, Mixer & Direct Digital Synthesizer (DDS) based AOM-driver 6
      1.2.7. Optical Cavity 7
      1.2.8. Recent Developments 7
   1.3. Research Question and PoR 8
      1.3.1. Research Question 8
      1.3.2. Program of Requirements (PoR) 8
      1.3.3. Scope of the Research 8
2. Experimental Method 9
   2.1. Materials and Setup 9
      2.1.1. Optical Path 10
      2.1.2. Electronic Path 10
      2.1.3. Digital PID Settings (Red Pitaya) & FM-deviation / LO-offset 11
      2.1.4. Analog PID Settings 11
      2.1.5. Measurement Protocol 12
3. Results 12
   3.1. Calibration 12
   3.2. Data Analysis 13
      3.2.1. Frequency noise and RMS calculation 13
   3.3. Digital (Red Pitaya) vs. Analog PID 14
   3.4. Final Results 15
4. Discussion 16
5. Conclusion and Recommendations 17
6. References 18
   6.1. AI Use 18
   6.2. Sources 18
7. Appendix 19
   7.1. List of Materials 19
   7.2. Photos 20
   7.3. Python code 25

1. Introduction

1.1. Background

In the SrMic Group at the UvA [18], the isotope ^{88}Sr is used for quantum computing and simulations, where they use the ultra-narrow atomic clock transition $^1S_0 \dashrightarrow {}^3P_0$. In this scheme the $^1S_0$ state is used as the logical **0** and the $^3P_0$ state is used as the logical **1**. This atomic transition is actually forbidden because of the 'selection' rules. (See *Figure 1* for the transitions in ^{88}Sr)

However, when a magnetic field is applied to the atoms, the selection rules are slightly relaxed because the field causes mixing between certain energy levels. This makes the originally forbidden transition weakly allowed [17].

They drive this transition using a 698 nm laser, as this is the required wavelength thus energy for this transition to occur. When laser light is continuously driving the atoms, this causes the probability amplitude to change continuously between the two states. This coherent evolution can be seen as a frequency that tells how fast this probability amplitude is changing between these two states. This is called the Rabi frequency [20]. In this case we talk about Rabi frequencies in the few kHz regime.

When there is laser light coming through an optical fiber there is phase/frequency noise being added to this light. If this noise is really significant around Fourier frequencies in this kHz regime and lower, this introduces errors into the quantum operations being executed [19].

These errors can be thought of as increasing the chance of "bit-flip-like" mistakes. When the laser has phase or frequency noise, it does not drive the atom exactly the way it should. As a result, the atom may not end up fully in the $^3P_0$ state, even though the quantum algorithm assumes it is there. Instead, part of the population can remain in the $^1S_0$ state. From the outside, this looks like a bit-flip error: the algorithm expects the qubit to be in the logical **1** state ($^3P_0$), but because of the noise, it might still be in the logical **0** state ($^1S_0$). So the frequency noise effectively increases the chance of ending up in the wrong state.

By implementing a fiber noise cancellation (FNC) system, the phase and frequency noise on the 698 nm laser is significantly reduced. As a result, the experimental errors in the ^{88}Sr quantum computing setup are significantly reduced, since the atoms experience a much more stable and coherent driving field during the quantum algorithm.

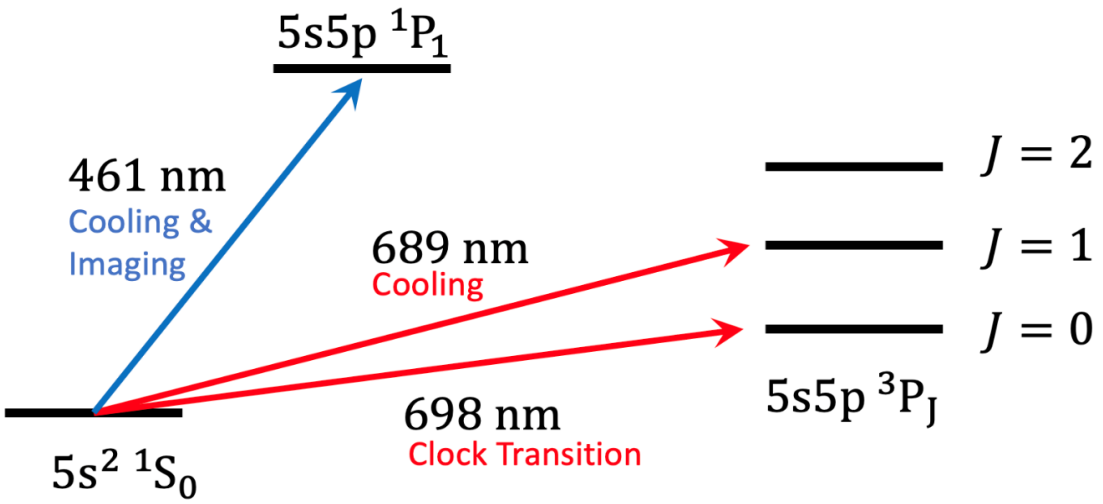


Figure 1: Energy levels and transitions of ^{88}Sr [17]

1.2. Theory

1.2.1. Fiber Noise

Fiber noise is phase/frequency noise that accumulates on laser-light when a laser-beam is travelling through an optical fiber [23]. Because of acoustic noise or temperature fluctuations, these varying conditions cause the optical path length to change over time, causing phase noise and thereby also frequency noise on the laser light. (See Equation 1 for the relation between frequency and phase) [2]

$$(\Delta f_0)(t) = \frac{1}{2\pi}\frac{d\phi(t)}{dt}$$

Equation 1

Here $(\Delta f_0)(t)$ is the frequency fluctuation and $\phi(t)$ is the phase fluctuation.

1.2.2. Beat-note

When a beat-note is made with two laser beams then what is done in essence is as follows: one of the two laser beams is shifted by ± 80 MHz, if they have the same polarization and are lined up perfectly on top of each other they will interfere, see Equation 2:

$$f_{beat} = |f_1 - f_2|$$

Equation 2

In this case we can say that f_1 is the laser beam that has been shifted by ± 80 MHz and f_2 has not. Then following the above equation a beat-note with a frequency of 80 MHz is created and this beat-note can now be measured using a photodiode and an oscilloscope/spectrum analyzer. This beat-note also contains all the information like the phase/frequency noise for example that is on the laser light. [6]

1.2.3. Power Spectral Density (PSD), Phase Noise & RBW / ENBW

The PSD of an arbitrary signal $x(t)$ expresses how the power is distributed over different Fourier frequencies [2]. In this case the spectrum analyzer gives the data in [dBm] at different Fourier-frequencies from the carrier. This dBm stands for decibel-milliwatts, this is a unit of power level expressed using a logarithmic decibel [dB] scale respective to one milliwatt [mW] [3]. In this case we only look at the positive frequencies, so one-sided. For future calculations we first convert the power from [dBm] to [mW] using Equation 3:

$$P_{mW} = 10^{\frac{P_{dBm}}{10}}$$

Equation 3

Then the PSD is calculated using Equation 4, where the PSD has the unit [mW/Hz].

$$PSD = \frac{P_{mW}}{ENBW}$$

Equation 4

ENBW stands for 'Equivalent Noise Bandwidth' with the unit [Hz], this is calculated by applying a dimensionless correction factor to the RBW (Resolution Bandwidth) depending on the used window function of the spectrum analyzer [4].

The RBW determines the ability to separate or resolve closely spaced signals, only if the RBW is smaller than the distance between two signals they can be resolved. Say two signals one at 100 Hz and the other at 150 Hz, if the RBW is smaller than the distance between these two signals (RBW = 10 Hz)

these two signals will be separated. But if the RBW is 100 Hz, then these signals will appear as a single signal in the trace. For more information about this or the spectrum analyzer in general, see this source [5].

There is also something called the linear single-sideband noise-carrier ratio $L(f)$ in [1/Hz] [2], this takes the single-sided PSD and normalizes it by dividing with the power of the carrier P_c using Equation 5. This quantity isn't the physical phase-noise spectral density yet but is necessary to eventually calculate the phase noise $S_\phi(f)$.

$$L(f) = \frac{PSD}{P_c}$$

Equation 5

The phase noise is calculated using Equation 6. The resulting $S_\phi(f)$ has units of $[\text{rad}^2/\text{Hz}]$, which corresponds to the phase variance per 1-Hz bandwidth [2]. The factor of two appears because $L(f)$ is defined as a single-sided quantity; therefore, to obtain the true two-sided phase-noise spectrum, this factor must be included.

The function $S_\phi(f)$ describes how much phase variance per 1-Hz band is present at a Fourier frequency f relative to the carrier frequency f_0. For example, consider a plot with Fourier frequency [Hz] on the x-axis and $S_\phi(f)$ $[\text{rad}^2/\text{Hz}]$ on the y-axis. If at a Fourier frequency of 100 Hz the value of $S_\phi(f)$is 1 rad^2/Hz, this means that the phase variance integrated over the 1-Hz band from 99.5 Hz to 100.5 Hz is equal to 1 rad^2.

$$S_\phi(f) = 2L(f)$$

Equation 6

1.2.4. Frequency noise & RMS

For the plots that will be used in this report, there has been made use of the frequency noise instead of the phase noise, see Equation 7 [2].

$$S_v(f) = f^2 S_\phi(f)$$

Equation 7

This is done by multiplying the phase noise $S_\phi(f)$ $[\text{rad}^2/\text{Hz}]$ with the square of the Fourier-frequency f. The unit of $S_v(f)$ is $[\text{Hz}^2/\text{Hz}]$, this means just the same as for the phase noise but then frequency variance instead of phase variance in a 1-Hz band at a specific Fourier frequency f.

Use has been made of the so called RMS frequency noise value σ_v of the frequency noise $S_v(f)$ $[\text{Hz}^2/\text{Hz}]$, calculated following Equation 8:

$$\sigma_v = \sqrt{\int_{f1}^{f2} S_v(f)df}$$

Equation 8

Here f_1 , f_2 determine the Fourier frequency band that we're integrating over and finding the RMS value of. In this case we will look at the 0 – 5 kHz band. The RMS value has the unit [Hz] and has the following physical meaning: The RMS frequency noise value that is calculated when there has been integrated over a Fourier frequency band of in this case 0 – 5 kHz, gives the 'amplitude' of how much

the carrier frequency f_0 fluctuates around its value caused by the frequency noise added by Fourier frequencies from 0 – 5 kHz, see *Equation 9*:

$$f(t) = f_0 + \Delta f(t)$$

Equation 9

Thus this value tells how much the beat-note frequency and thereby also the laser frequency is fluctuating on average over time.

1.2.5. Acousto Optical Modulator (AOM), Polarizing Beam Splitter (PBS) & Faraday Isolator (FI)

AOM:
An AOM is essentially a transparent crystal (e.g., glass) on which an acoustic wave is imposed using a piezoelectric transducer driven by an RF signal, for example around 100 MHz. This acoustic wave creates a traveling strain field in the crystal. Through the photo-elastic effect, this strain forms a moving refractive-index grating that causes Bragg diffraction of the incident light. As a result, multiple diffraction orders are being created: the 0^{th} order remains unshifted in frequency, while the $\pm 1^{st}$ orders are shifted by ±100 MHz, corresponding to the applied RF frequency. See source [7] for more information on AOMs.

PBS:
A PBS (polarizing beam splitter) is an optical component that separates an incoming beam into two paths based on polarization. When unpolarized light enters a PBS, it is split into its S-polarized and P-polarized components. P-polarized light is usually transmitted straight through, while S-polarized light is reflected by 90°. The device can also be used in reverse to combine two beams for interference. By preparing the input polarization as either S or P, one can choose whether the beam is transmitted or reflected. See source [8] for more information about PBSs

FI:
A Faraday isolator is an optical device that makes sure light can only travel in one direction. It is mainly used to protect lasers from back-reflected light, which can cause noise or even destabilize the laser. A Faraday rotator rotates the polarization of the incoming light by usually 45° using a strong magnetic field. Because this rotation is non-reciprocal (it does not reverse when light travels backward), the device functions as an isolator when the rotator is combined with two PBSs, in this case:

- light going forwards passes through with little loss,
- light coming backwards is rotated into the “wrong” polarization and is almost completely reflected by typically 90°.

This way, any light reflected back from the optical setup cannot enter the laser again. For more information see source [9].

1.2.6. Red Pitaya, Mixer & Direct Digital Synthesizer (DDS) based AOM-driver

Red Pitaya:
A Red Pitaya (RP) is a compact, open-source, FPGA-based board for high signal acquisition and processing (See this source for more information about the RP [12]). It can be used as an oscilloscope, signal generator, spectrum analyzer etc.. Together with the use of the ‘PyRPL software’ the RP can also be used as a digital PID controller. (See this source for more information about PyRPL [13]). For pictures of the user interface see *Figure 15* & *Figure 16*.

Mixer:
An (RF) mixer works as follows, it mixes two RF-signals and thereby creates two output RF-signals:

$$f_{out,1} = f_{in,1} + f_{in,2}$$

Equation 10

$$f_{out,2} = f_{in,1} - f_{in,2}$$

Equation 11

As can be seen in *Equation 10* & *Equation 11* one of these output signals is the sum of the two input signals and the other one is the difference of the two input signals. If this mixer is combined with for example a high-pass or low-pass filter it can be determined which one of these output signals will be extracted. (See this source for more information about mixers [*14*])

DDS based AOM-driver:
The Direct Digital Synthesizer (DDS) is the chip inside the AOM-driver that generates the RF signal used to drive the AOM. It creates an analog waveform—usually a sine wave—by first producing the signal digitally and then converting it to an analog output using a digital to analog converter (DAC). Because the DDS is digitally controlled, it can switch frequencies very quickly and with high precision. This makes it ideal for applications such as fiber noise cancellation (FNC), where rapid phase and frequency corrections are needed to compensate for the noise that the laser light picks up while traveling through the optical fiber. (See this source for more information about DDS [*15*])

1.2.7. Optical Cavity

A linear optical cavity typically consists of two partially transparent mirrors facing each other. One mirror lets a small amount of light into the cavity (the input coupler), and the other lets a small amount of light out (the output coupler). Once the light is inside, it bounces back and forth many times between the mirrors.

Because only certain wavelengths fit an integer number of half-wavelengths between the mirrors, the light forms standing waves, also called cavity modes. This is similar to how a guitar string only vibrates at certain resonant frequencies. The same idea applies to the electromagnetic field inside the cavity.

Together with a feedback loop, the laser can be locked to one of the cavity modes. This forces the laser to follow the resonance frequency of the cavity as best as it can. As a result, the laser frequency becomes much more stable, and the phase/frequency noise is reduced by a few orders of magnitude at the relevant Fourier frequencies. (See source [*11*] for more detailed information)

1.2.8. Recent Developments

The FNCS-1000-1 Fiber Noise Cancellation System from Stable Laser Systems is a modern device designed to suppress unwanted noise in optical fibers [*21*]. This is especially important in applications such as experiments with ^{88}Sr, where 698 nm lasers are used and maintaining a highly stable signal is crucial for precise measurements. The system combines digital phase detection with an FPGA-based servo controller, allowing it to effectively reduce both phase and intensity noise. Its compact design and user-friendly interface also make it easy to integrate into laboratory setups. Although the exact release date is not publicly documented, the FNCS-1000-1 is part of the latest generation of systems for distributing frequency-stabilized light through optical fibers, aligning with current trends in quantum technology and precision timing.

The cost of this commercial FNC system is quite high—approximately $10,000 (based on a received quote). Although FNC systems are important for quantum experiments, this price is too high for a single piece of equipment for a university with a more limited budget compared to most industrial companies. Therefore, it would be preferable to build this system ourselves at a lower cost.

1.3. Research Question and PoR

1.3.1. Research Question

The main research question of this study is:

How can a fiber noise cancellation (FNC) system be designed and implemented to suppress the frequency noise accumulated by 698 nm laser light during optical fiber transmission, and how can its effectiveness be analyzed using beat-note and frequency noise PSD ($S_v(f)$) plots?

Important note:
Because this project focuses on the design and construction of an FNC system, the research question is addressed primarily in the '*Experimental Method*' section (2). The '*Results*' section (3) then presents the plots and data that demonstrate the effectiveness of the implemented system.

1.3.2. Program of Requirements (PoR)

Functional Requirements:

1. The system must suppress frequency noise by at least 20 dB at Fourier frequencies in the range of 0 – 1 kHz for an optical fiber of approximately 30 meters long.

Test Conditions:

1. Comparative tests will be carried out between two PID implementations:
   (a) Digital PID (Red Pitaya) and
   (b) Analog PID (Workshop).

Objective:
The objective of this system is to suppress the frequency noise caused by the optical fiber as much as possible, so that the laser light remains suitable for experiments in the other lab. The test conditions will be evaluated using identical measurement procedures, allowing the performance to be compared objectively.

1.3.3. Scope of the Research

This research focuses on the design and implementation of a fiber noise cancellation (FNC) system for laser light with a wavelength of 698 nm in a laboratory setup. The goal is to actively suppress frequency noise caused by optical fibers, using components such as an AOM, photodiode, PI(D) controller, and DDS. The effectiveness is measured through frequency-noise analysis (S_v-spectrum) and the RMS frequency-noise value for Fourier frequencies from 0–5 kHz. Factors such as other lasers, commercial FNC systems, and other atomic processes lie outside the scope of this study.

The investigated FNC system is implemented as a proof of concept for one specific application. Although the system must be used several times in slightly different configurations in experiments at the UvA laboratories, this research is limited to discussing a single system and its corresponding results, in order to demonstrate feasibility and effectiveness.

2. Experimental Method

2.1. Materials and Setup

For the full list of materials, please see the sub-section *"List of Materials (7.1)"* in the appendix. Below are two figures: a photo of the actual setup and a schematic drawing of the setup. The other photos have been moved to the sub-section *"Photos (7.2)"* in the appendix. For the legend showing the meaning of the abbreviations see *Figure 3*. Not all the component labels are shown in the photo, this is mainly to keep things clear, without it getting too messy.

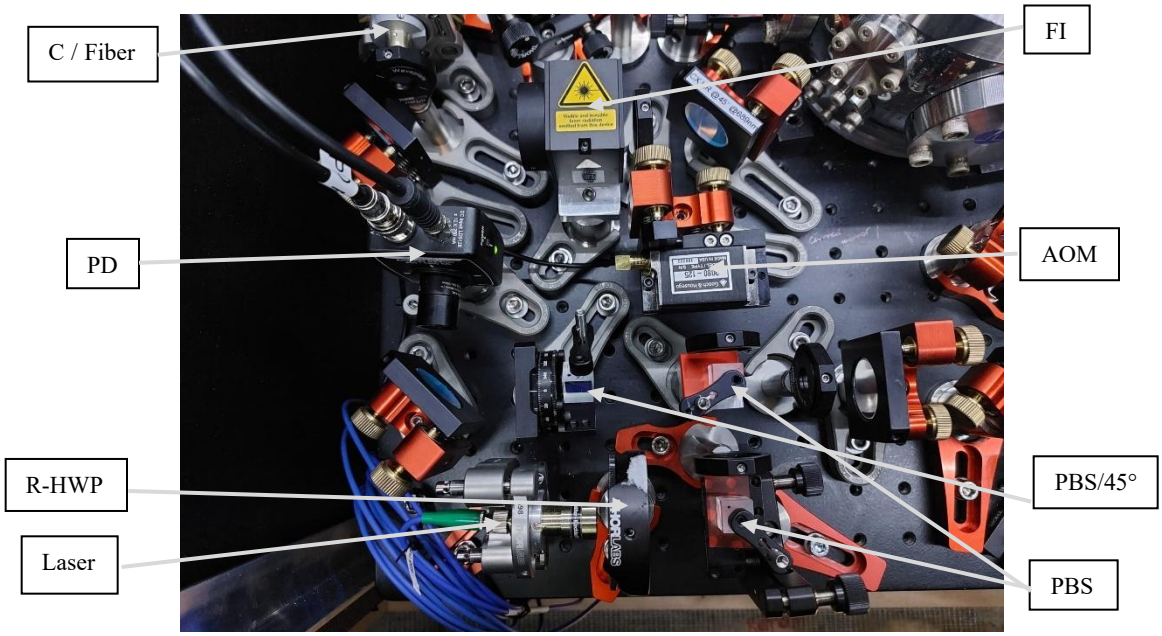


Figure 3: Photo of the optical setup

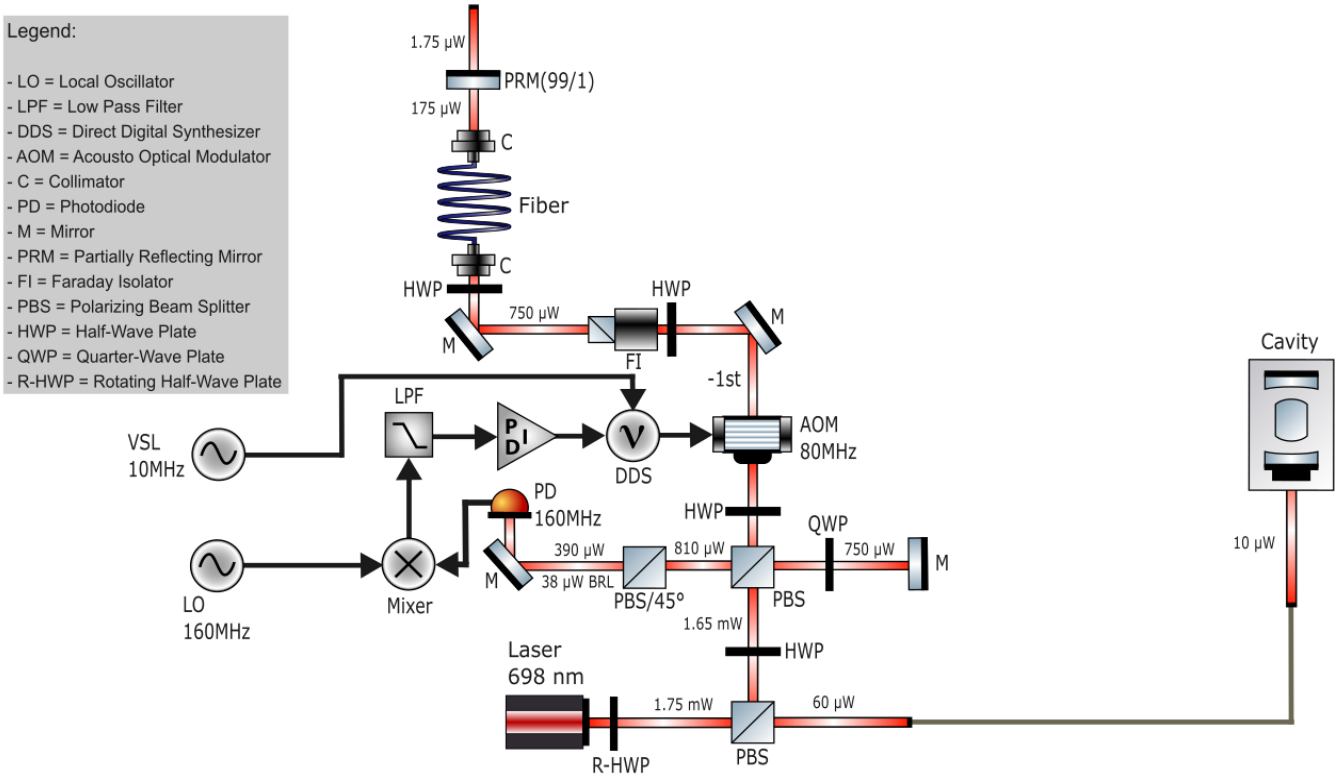


Figure 2: Schematic drawing of the setup (created by myself using Inkscape)

2.1.1. Optical Path

Figure 2 shows a complete schematic of the full FNC setup, including optical powers in some paths. We describe the setup step by step to understand its operation. (The optical powers have been included because these are important for reproducibility)

The system starts with the 698 nm laser, shown in *Figure 3* as the blue fiber at the bottom. The laser light first passes through a rotating half-wave plate (R-HWP) to set its linear polarization, controlling the power directed to the FNC setup and toward the cavity via the first polarizing beam splitter (PBS), where ~1.75 mW is measured. After splitting, ~60 µW goes to the cavity, while 1.65 mW continues to the FNC setup through another HWP. (For the settings of the laser source boxes, see *Figure 14*)

At the second PBS, the light divides into two paths. One path is reflected through a quarter-wave plate (QWP) and a mirror, carrying ~750 µW. The other path continues through a HWP into the acousto-optic modulator (AOM), where it is frequency-shifted by -80 MHz using the -1st diffraction order; other orders remain unused. The light then passes a HWP and enters the Faraday Isolator (FI) to shift its polarization by 45° and prevent back-reflected light from re-entering the laser. After the FI, ~750 µW remains (all diffraction orders), with only the -1st order coupled into the fiber with a HWP in front for polarization-maintaining.

On the far side of the 35-meter fiber, ~175 µW is present; 99% is reflected back and 1% (1.75 µW) is transmitted. This transmitted light serves as the "clean" light for subsequent optical setups and the experiment. (See *Figure 13*)

The back-reflected light retraces the optical components in reverse and recombines with the reference beam at the third PBS, set at 45° to maintain polarization for interference. About 810 µW enters this PBS, leaving ~390 µW afterward (all diffraction orders). The back-reflected light (BRL) has ~38 µW, measured by blocking the reference beam.

This BRL, having double-passed the fiber and AOM, accumulates twice the fiber-induced frequency noise and a total shift of -160 MHz. It interferes with the reference beam, which lacks the fiber-induced noise and the frequency shift. The resulting interference is detected by the photodiode (PD), producing a 160 MHz beat-note that carries the frequency noise information.

2.1.2. Electronic Path

The RF signal made by the PD is DC-blocked and then mixed with a 160 MHz signal from the local oscillator (LO), producing two outputs: one at 320 MHz and one near DC, which contains only the relatively slow frequency noise. These signals pass through a low-pass filter (LPF) that allows only frequencies from DC to 2.5 MHz, isolating the desired signal. This filtered signal serves as the error signal for the PID controller, which can be either analog or digital (Red Pitaya). See *Figure 8* & *Figure 9*. The PID controller compares the error signal to a setpoint—0 V for the analog PID and -0.027 V for the Red Pitaya—chosen at the most linear portion of the sine wave for maximum sensitivity. The controller then adjusts its output to minimize the difference, driving the error signal toward the setpoint.

The PID output is connected to the frequency modulation (FM) port of the AOM-driver (DDS). The voltage from the PID is converted into additional frequency modulation on the laser light passing through the AOM, modulating around the constant 80 MHz shift. This compensates for the phase—or equivalently, frequency—noise accumulated by the light in the fiber. See *Figure 10*. At last, the 'VSL 10 MHz' is an reference RF-signal at 10 MHz used for the DDS, to reduce the amount of phase/frequency noise that the AOM induces on the laser-light.

2.1.3. Digital PID Settings (Red Pitaya) & FM-deviation / LO-offset

When using the Red Pitaya (RP) see *Figure 11*, calibration was required because the device had been modified to output 0–2.2 V instead of the standard –1 to +1 V. Consequently, a constant 1 V offset had to be applied to the FM port of the DDS to allow the RP to compensate both positive and negative error-signal deviations and drive the signal toward the setpoint.

The DDS provides an FM-deviation setting that determines the frequency modulation per volt. For the comparison between the RP PID and the analog PID, a value of 3200 Hz/V was used. However, because of the impedance mismatch between the RP (50 Ω) and the DDS (1 kΩ), this value did not correspond to the actual effective modulation, necessitating calibration when using the digital (RP) PID.

Due to the constant 1 V offset at the FM port, the laser frequency was continuously modulated by 800 Hz. To obtain a clean near DC error signal, the local oscillator also needed to include this 800 Hz offset. The origin of this 800 Hz value will be clarified in the sub-section *3.1*.

After applying both the Ziegler–Nichols method [*16*] and manual fine-tuning, the optimal PID parameters for this configuration were found to be: **P = 2048, I = 38 856, and D = 0**, meaning the controller effectively operated as a PI controller. The P and I values were at the maximum allowed by the software.

2.1.4. Analog PID Settings

The analog PID operated differently from the Red Pitaya. Its settings were adjusted using switchable coarse-gain selectors and fine-tuning trim-pots (see *Figure 4*). While observing the signal on the spectrum analyzer, I adjusted these controls to minimize the noise floor, maximize the signal peak, and push the servo bumps as far from the carrier as possible (see *Figure 12*). After optimization, the following settings were used:

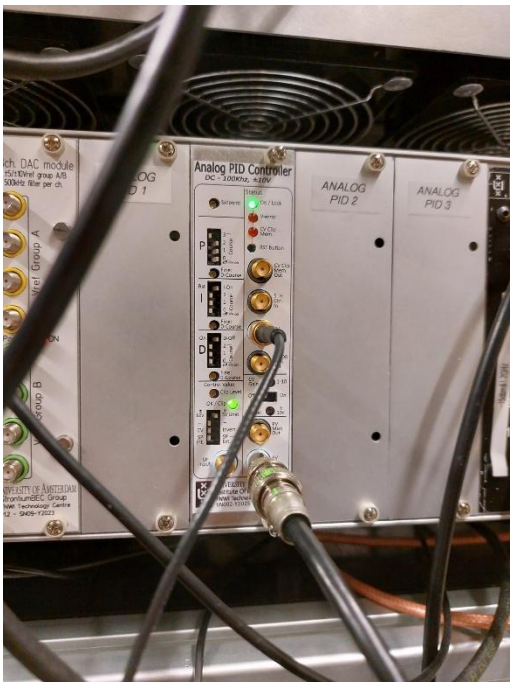


Figure 4: Analog PID

P-gain: All switches on (to the right) except the top one; the P trim-pot set to its maximum value (fully clockwise).

I-gain: All switches off; the I trim-pot adjusted so the servo bumps appeared at the highest possible Fourier frequency from the carrier (42 kHz in this case).

D-gain: All switches off; the D trim-pot minimized.

The CV gain trim-pot, which sets the minimum and maximum output voltage, was adjusted while monitoring a multimeter and set to ±9.2 V. This ensured the output stayed within the ±10 V input range of the DDS and prevented overload.

Finally, the module included an error-gain setting, adjustable via jumpers on internal pins. According to the provided documentation, this was set to 100×. Since the error gain scales linearly with the PID parameters, increasing it effectively expanded the available PID range. (See *Table 1*)

2.1.5. Measurement Protocol

Measurements were taken using the R&S FSH8 Spectrum Analyzer (SA) (see again *Figure 12*). The photodiode output was connected to the SA, and the instrument was configured with the following settings:

- **Span:** 25 kHz (Fourier frequency range scanned)
- **Center frequency:** 160 MHz (the beat-note frequency)
- **RBW / VBW:** 3 Hz (resolution and video bandwidths)
- **Trace mode:** Averaging ×10 (computes the mean of 10 sweeps for improved reliability)
- **Detection:** Max Peak (records the maximum power in [dBm] at each Fourier frequency)

With these settings, one sweep took approximately 27.5 seconds, giving a total measurement time of roughly 275 seconds (4 minutes 35 seconds) per averaged trace. I recorded 10 measurements with the FNC loop off and 10 with the loop on—20 measurements in total—resulting in a total acquisition time of about 1 hour and 32 minutes.

The data were extracted via USB and converted from SET to CSV format using the SA's software [22]. These CSV files were subsequently used for further analysis.

3. Results

3.1. Calibration

To determine the actual FM-deviation, a calibration was performed by setting specific voltages in the 'PyRPL software'—which interfaces with the Red Pitaya—and observing the resulting carrier-frequency shift on the spectrum analyzer. This produced multiple data points, from which a linear fit was made on a graph with frequency modulation [Hz] on the y-axis and 'PyRPL voltage [V]' on the x-axis (see *Figure 5*).

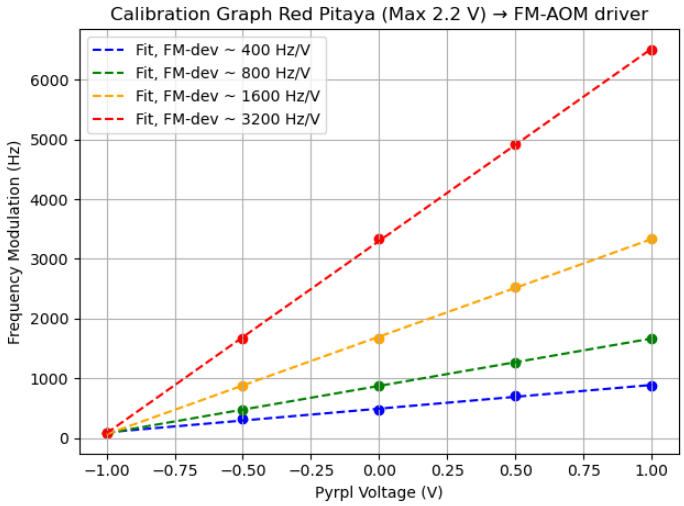


Figure 5: Calibration Graph

Because the Red Pitaya had been modified, the 'PyRPL voltage' did not correspond directly to the physical output voltage: −1 V in PyRPL corresponded to 0 V on the RP, 0 V corresponded to 1 V, and +1 V corresponded to about 2.2 V. As visible in the calibration plot, the slope of each line was approximately twice that of the previous one.

As noted earlier, the effective FM-deviation when the DDS (AOM-driver) was set to 3200 Hz/V differed substantially from the nominal value. The blue line in *Figure 5* corresponds to this case and shows an actual FM-deviation of roughly 400 Hz/V.

The local oscillator (LO) required a frequency of 160 MHz + 800 Hz because the 400 Hz deviation is the modulation produced by a single pass through the AOM, whereas the light undergoes a double pass before reaching the photodiode. Since the 'PyRPL voltage' must be set to 0 V (which corresponds to 1 V on the RP hardware), the laser always carries this constant 800 Hz modulation. To cancel it, the LO must include the same 800 Hz offset.

3.2. Data Analysis

3.2.1. Frequency noise and RMS calculation

This section explains how the raw spectrum-analyzer data—recorded as power [dBm] versus Fourier frequency [Hz]—was processed to obtain the frequency-noise spectra [Hz²/Hz] and the RMS frequency noise [Hz]. The procedure follows the Python workflow shown in sub-section (*7.3*).

After loading the CSV files with Pandas and extracting the Fourier frequency and power columns, the data are processed within a dedicated function. The power values are first converted from [dBm] to [mW] to work with linear units rather than logarithmic ones.

The carrier is located by applying 'argmax' to the linear-power array; this yields both the carrier frequency and its power. To normalize the spectrum, the sum of 20 points surrounding the carrier is used. Since the nearby data points are much lower in power, this approach is straightforward and sufficiently accurate.

Only the positive (one-sided) Fourier frequencies are retained, following the theory described in Section *1.2*. This is done by subtracting the carrier frequency from all frequency values, then masking to keep only the positive frequencies and their corresponding powers.

Next, the Equivalent Noise Bandwidth (ENBW) is computed by applying a correction factor to the RBW that depends on the window function used by the spectrum analyzer. Because the analyzer's window type was not specified, an ENBW correction factor of 1 was assumed. The power spectral density (PSD) is then calculated simply as the power [mW] divided by the ENBW [Hz].

The linear single-sideband noise-carrier ratio [1/Hz] is obtained by dividing the PSD in [mW/Hz] with the normalized carrier power (also in [mW]). From here, the known relation between L_{lin} and phase noise (S_ϕ) is used to compute the phase-noise spectrum [rad²/Hz], and the corresponding relation between phase noise and frequency noise (S_v) yields the frequency-noise spectrum [Hz²/Hz].

Finally, although not shown in the code, the RMS frequency noise from 0–5 kHz is calculated using *Equation 8*, numerically integrating the frequency-noise spectrum with the trapezoidal method. (See source [*10*] for information about the trapezoidal method)

3.3. Digital (Red Pitaya) vs. Analog PID

After extensive characterization of both the digital and analog PID controllers, it was found that setting the FM-deviation on the DDS to 3200 Hz/V provided the most effective noise reduction in the lower Fourier frequency range of interest. See *Figure 6* for the results:

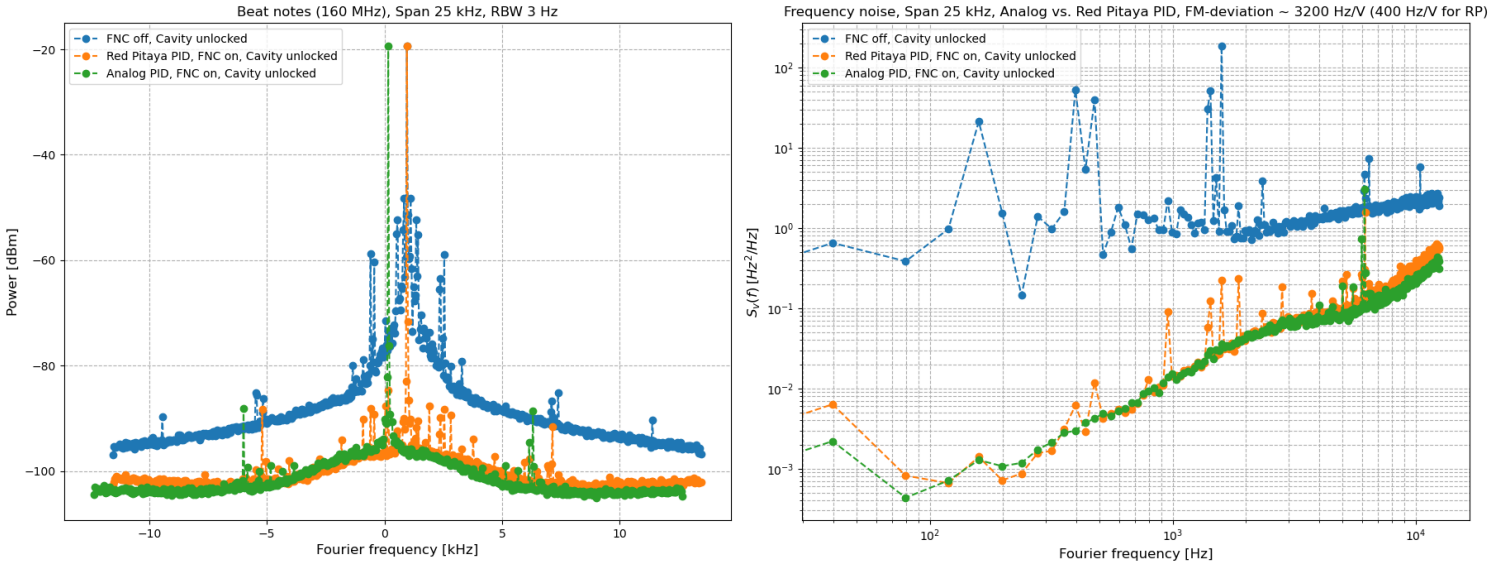


Figure 6: Digital vs. Analog PID plots

These measurements were taken using a very short fiber (few meters), compared to the fiber used in the setup that has been explained in the experimental method of 35 meters long.

In the left plot, the raw data directly from the spectrum analyzer are shown: the y-axis displays the power in [dBm], and the x-axis shows the Fourier frequencies in [kHz]. The Fourier frequency of 0 kHz corresponds to the 160 MHz beat-note, which is why the peak appears so prominently at this point. (The blue and orange trace peaks are shifted by 800 Hz as mentioned before) The right plot shows the corresponding frequency-noise spectrum, with units of [Hz²/Hz] on the y-axis and Fourier frequency [Hz] on the x-axis; both axes are logarithmically scaled, in contrast to the linear axes used in the other plot.

In the left plot, it can be seen that the blue trace has a much wider peak around its center frequency than the other two traces, and the noise floor is also higher. This is due to the presence of significantly more low-frequency noise when the FNC system is switched off. In short, a narrower peak and a lower noise floor indicate better performance in this case. The left plot essentially shows the Fourier transforms of the acquired RF signals. In the right plot (frequency-noise PSD), lower values indicate better performance, especially in the 0–5 kHz Fourier frequency range.

As indicated in the plot labels, the cavity was unlocked during these measurements. This results in a slightly elevated noise floor compared to a locked-cavity case. In both plots, it is evident that enabling the FNC system (orange and green traces, corresponding to the digital and analog PID, respectively) significantly lowers the noise floor compared to the FNC-off case (blue). A closer comparison between the digital PID (orange) and the analog PID (green) shows that the analog controller exhibits far fewer peaks in the ~400 Hz to ~4 kHz range, suggesting that the analog PID introduces less electronic noise then its digital counterpart. This is further supported by the RMS values calculated over the 0–5 kHz Fourier frequency range: approximately 17.0 Hz for the digital PID and 15.5 Hz for the analog PID. Although no standard error is shown for these values, each spectrum represents an internal 10× average on the spectrum analyzer, as described in the experimental methods. Only one trace per condition has been measured here, because this was part of the characterization process. Considering both the plotted data and the RMS values, it was concluded that the analog PID was the preferable choice for the present application.

3.4. Final Results

With all of the characterization and optimizations done, the final measurements were taken following the '*Measurement Protocol* (2.1.5)'. See *Figure 7* for the results:

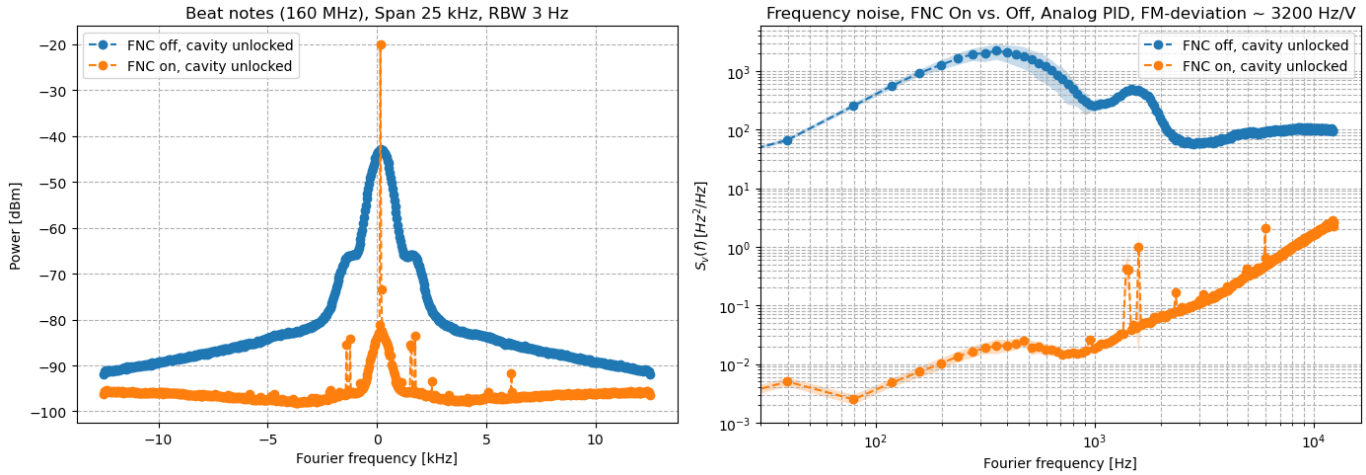


Figure 7: Final results

As shown, the noise level with the FNC system off increases substantially compared to the previous plot. This is because these measurements were taken using the longer 35 m fiber that runs across the hallway into another lab, making it more sensitive to temperature fluctuations and acoustic disturbances. In the left plot (beat-note spectrum), two bumps appear around –65 dBm in the blue trace (FNC off), and although they are still visible in the orange trace (FNC on), they are strongly suppressed. These features likely originate from a relatively strong acoustic noise source near ~1500 Hz, such as a fan, pump, or other laboratory equipment. Also a noise reduction of approximately 30 dB can be noticed at Fourier frequencies from 0 to 1 kHz in this plot.

In the right plot, the frequency-noise reduction is even more pronounced then in the earlier measurement. At very low Fourier frequencies (tens to hundreds of Hz), the noise suppression reaches a factor of ~10^5, demonstrating that the FNC system performs extremely well in this range. Note that the cavity remained unlocked during these measurements; locking it would further reduce the absolute noise level.

The shaded regions in the right plot show the standard deviation of the ten repeated measurements for both the FNC-off and FNC-on traces.

From the RMS values and their standard errors (0–5 kHz range), we find:

- **FNC off (blue): RMS = 1262.0 ± 49.0 Hz**
- **FNC on (orange): RMS = 24.98 ± 0.37 Hz**

Thus, the FNC system reduces the RMS frequency noise in the 0–5 kHz Fourier frequency band by approximately a factor of 50.

4. Discussion

Comparing the obtained results with the functional requirements stated in the sub-sub-section *Program of Requirements (PoR)* (*1.3.2*) the following can be said:
These requirements specified that:

1. The FNC system must suppress frequency noise by at least 20 dB within the 0–1 kHz Fourier frequency range for an optical fiber of approximately 30 meters long.
2. A comparison between a digital and an analog PID controller must be performed.

From the results presented in Section *3*, all of these requirements have been successfully met.
First, the noise suppression achieved in the 0–1 kHz range, as shown in the *Final Results* sub-section (*3.4*), exceeds the requirement significantly, reaching approximately 30 dB of suppression.
Second, the final measurements were carried out using a 35 m fiber, fulfilling the requirement regarding the operational fiber length.

Finally, a comparison between the digital and analog PID controllers was performed (Section *3.3*: *Digital (Red Pitaya) vs. Analog PID*), where it was concluded that the analog PID controller is the better choice for this application.

Next, there is a different FNC system described in a Master's thesis by Anders Rönnholm (Lund University) [*1*], where a noise reduction of over 10 dB was achieved up to 20 kHz Fourier frequency.

We can therefore conclude that our current system is significantly more effective at suppressing noise in the lower Fourier-frequency range then at higher frequencies. This is exactly what was intended, since noise in the 0–5 kHz range has the strongest impact on the experiment and is therefore the most important to reduce.

Furthermore, regarding the statistical reliability of the measurements: each trace recorded by the spectrum analyzer included an internal 10× averaging, already reducing the standard deviation. In addition, 10 individual measurements were performed for each condition (FNC on and FNC off). This not only further decreased the statistical uncertainty, but also captured more natural variations in the setup—such as laser-power fluctuations, acoustic disturbances, and temperature drifts—providing insight into the system's long-term stability over time scales on the order of ~1.5 hours. Such stability is essential for future experiments that require extended measurement durations.

Lastly, these measurements were performed using the in-loop photodiode. This means the results primarily show how effectively the FNC system suppresses noise inside the feedback loop, based on the beat signal formed by the reference beam and the light returned through the fiber. Because this detector is part of the servo loop, the measured frequency noise does not represent the true stability of the light delivered to the experiment.

For a more realistic performance evaluation, an out-of-loop measurement is required. In that case, the beat-note is formed between the laser and the actual "science light" seen by the atoms—such as the ~1.75 µW transmitted through the partially reflecting mirror at the remote end of the fiber. The frequency noise obtained from this out-of-loop photodiode provides a much more accurate estimate of the final laser stability relevant for the atomic experiment.

If this is not feasible, it may be preferable to perform the experiment with the ^{88}Sr atoms both with the fiber noise cancellation (FNC) loop disabled and enabled, and to compare the two cases. This comparison is likely to provide the most accurate and reliable indication of the FNC performance in the atomic experiment.

Nevertheless, the results in this document still show the effectiveness of the FNC system.

5. Conclusion and Recommendations

Conclusion:

The aim of this project was to evaluate whether the developed Fiber Noise Cancellation (FNC) system meets the stability requirements for transferring a low-noise optical signal through a ~30 m fiber, and to determine whether an analog or digital PID controller provides the best performance. The results clearly show that the system meets all predefined requirements.

The measured noise suppression exceeds 20 dB in the 0–1 kHz Fourier frequency range, and the RMS frequency noise is reduced from **1262.0 ± 49.0 Hz** (FNC off) to **24.98 ± 0.37 Hz** (FNC on), corresponding to an improvement of approximately a factor of 50 in the 0–5 kHz range using an analog PID controller.

These results demonstrate that the implemented FNC system is highly effective, especially in the very low-frequency region where the noise reduction reaches a factor of $\sim 10^5$. Based on these findings, the overall design expectations are fully confirmed.

Recommendations for improving the method:

Several improvements could further increase the accuracy and reliability of the measurements:

- Increase spectrum averaging (e.g., 100× instead of 10×) while maintaining an RBW of 3 Hz to reduce measurement uncertainty, acknowledging the longer acquisition time.
- Use the ENBW instead of the RBW when calculating the PSD, if the correction factor of the used window function is known.
- Perform measurements with the cavity locked, matching the intended operating conditions of the 698 nm laser system.
- Use an out-of-loop photodiode at the far end of the fiber to evaluate the actual light seen by the atoms, providing a more representative stability measurement. Alternatively, perform the experiment with the ^{88}Sr atoms both with the fiber noise cancellation (FNC) loop enabled and disabled. Comparing these two cases would provide a direct and reliable assessment of the FNC loop performance and its impact on the atomic experiment.

Suggestions for follow-up research:

A logical next step would be to implement the improvements listed above and repeat the measurements to verify whether the system's performance can be characterized with higher precision. In addition, the same FNC architecture could be evaluated for other laser wavelengths used within the laboratory. This follow-up research could consist of (1) adapting AOM and electronic components to the new wavelength, (2) characterizing the free-running fiber noise for that system, and (3) re-optimizing the PID parameters for the new optical configuration. This would help broaden the application of the FNC technique and improve stability across multiple experiments.

6. References

6.1. AI Use

The texts of this report were reviewed and refined using ChatGPT (OpenAI), an AI-based language assistant. The tool was used exclusively to support spelling, grammar, and formulation improvements. Prompts such as: *"Correct the spelling, grammar, and formulation of this text: ..."* were used for this purpose.

6.2. Sources

1. [1] A. Rönnholm, "Fiber noise cancellation," Lub.lu.se, 2025. https://lup.lub.lu.se/student papers/search/publication/2834772 (accessed Dec. 02, 2025).
2. [2] E. Rubiola, "Enrico Rubiola Phase Noise Phase Noise and Frequency Stability," 2024. Accessed: Nov. 28, 2025. [Online]. Available: https://rubiola.org/pdf-lectures/Scient-Instrum-Files/Phase%20noise%2C%20incremental%20notes%20based%20on%20Ch2.pdf?
3. [3] Wikipedia Contributors, "dBm," *Wikipedia*, Sep. 17, 2018. https://en.wikipedia.org/wiki/DBm
4. [4] Mathuranathan, "Equivalent noise bandwidth (ENBW) of window functions – GaussianWaves," Gaussianwaves.com, Sep. 13, 2020. https://www.gaussianwaves.com/2020/09/equivalent-noise-bandwidth-enbw-of-window-functions/? (accessed Oct. 03, 2025).
5. [5] Rohde, "Understanding basic spectrum analyzer operation," *Rohde-schwarz.com*, 2024. https://www.rohde-schwarz.com/nl/products/test-and-measurement/essentials-test-equipment/spectrum-analyzers/understanding-basic-spectrum-analyzer-operation_256005.html
6. [6] D. R. Paschotta, "Beat Note," *www.rp-photonics.com*. https://www.rp-photonics.com/beat_note.html
7. [7] D. R. Paschotta, "Acousto-optic modulators," *www.rp-photonics.com*. https://www.rp-photonics.com/acousto_optic_modulators.html
8. [8] "MEETOPTICS | Search & Compare Quality Optics," *Meetoptics.com*, 2025. https://www.meetoptics.com/academy/polarizing-beamsplitters
9. [9] D. R. Paschotta, "Faraday Isolators," *www.rp-photonics.com*. https://www.rp-photonics.com/faraday_isolators.html
10. [10] RMIT Library, "NM3: The trapezoidal rule - Learning Lab - RMIT University," *Learning Lab - RMIT University* -, Oct. 16, 2023. https://learninglab.rmit.edu.au/maths-statistics/numerical-methods/nm3-trapezoidal-rule/
11. [11] D. R. Paschotta, "Optical Resonators," *www.rp-photonics.com*. https://www.rp-photonics.com/optical_resonators.html
12. [12] "STEMlab 125-14 - Red Pitaya," *Red Pitaya*, Jun. 07, 2021. https://redpitaya.com/stemlab-125-14/?srsltid=AfmBOooVA6rpFwQ2Yj4rW9ReqUyZy8IXjZiTkCOrXIrD_rFTcE1fs62Z (accessed Dec. 04, 2025)
13. [13] L. Neuhaus *et al.*, "Python Red Pitaya Lockbox (PyRPL): An open source software package for digital feedback control in quantum optics experiments," *Review of Scientific Instruments*, vol. 95, no. 3, Mar. 2024, doi: https://doi.org/10.1063/5.0178481.
14. [14] "The Basics of Mixers," *www.digikey.com*. https://www.digikey.com/en/articles/the-basics-of-mixers
15. [15] "All About Direct Digital Synthesis | Analog Devices," *Analog.com*, 2024. https://www.analog.com/en/resources/analog-dialogue/articles/all-about-direct-digital-synthesis.html
16. [16] Wikipedia Contributors, "Ziegler–Nichols method," *Wikipedia*, Apr. 22, 2019. https://en.wikipedia.org/wiki/Ziegler%E2%80%93Nichols_method
17. [17] Q. Light, "Sr Quantum Clock," Durham QLM, 2024. https://durham-qlm.uk/research/rydberg/strontium/ (accessed Sep. 05, 2025).

18. [18] “StrontiumBEC,” *Strontiumbec.com*, 2025. https://www.strontiumbec.com/ (accessed Dec. 05, 2025).
19. [19] X. Jiang, J. Scott, M. Friesen, and M. Saffman, “Sensitivity of quantum gate fidelity to laser phase and intensity noise,” *Physical review. A/Physical review, A*, vol. 107, no. 4, Apr. 2023, doi: https://doi.org/10.1103/physreva.107.042611.
20. [20] D. R. Paschotta, “Rabi oscillations,” *www.rp-photonics.com*. https://www.rp-photonics.com/rabi_oscillations.html
21. [21] “Fiber Noise Cancelation System - Stable Laser Systems,” *Stable Laser Systems*, Dec. 05, 2023. https://stablelasers.com/products/fiber-noise-cancelation-system/
22. [22] “Download FSH4View by Rohde & Schwarz GmbH & Co. KG,” *Informer.com*, 2021. https://fsh4view.software.informer.com/download/ (accessed Jan. 14, 2026).
23. [23] Coherent, “What are Fiber Optics and How Do They Work? | Coherent,” www.coherent.com, 2024. https://www.coherent.com/news/glossary/optical-fibers

7. Appendix

7.1. List of Materials

Below is the list of materials used during this project. Standard optical setup hardware such as mirror mounts, screws and posts has been omitted for brevity:

Materials:	Company:	Specifics:	Amount:
DDS 500 MHz LO	UvA IOP FNWI Technology Center	500 MHz (max range) Local Oscillator	1
Analog PID Controller	UvA IOP FNWI Technology Center	DC - 100 kHz, ± 10 V	1
BNC cables	Thorlabs	50 Ohm Impedance	3
SMA cables	Thorlabs	50 Ohm Impedance	3
SMA (f) - BNC (m) adapter	Thorlabs	50 Ohm Impedance	1
SMA (m) - BNC (f) adapter	Thorlabs	50 Ohm Impedance	1
DC-block	Mini-Circuits	BLK-89-S+ (for LO signal)	1
BNC (m) to SMA (m) cable	Thorlabs	50 Ohm Impedance	1
VSL 10 MHz RF-signal	Dutch Metrology Institute	10 MHz Reference signal for AOM-driver	1
Red Pitaya PID Controller	Red Pitaya	STEMlab-125-14 (modified)	1
AOM-driver (DDS)	Time-Base.de	AOM-Driver DIM-3000	1
Mixer	Mini-Circuits	ZAD-1-1+	1
BNC T-splitter	Thorlabs	50 Ohm Impedance	1
Low Pass Filter (LPF)	Mini-Circuits	BLP-2.5+ (for output mixer 'Error-signal')	1
DC-block	Mini-Circuits	BLK-222+ (for input photodiode into mixer)	1
Oscilloscope	RIGOL	DS1054Z	1
Spectrum Analyzer	Rohde & Schwarz	FSH8	1
Power Meter	Thorlabs	PM100D	1
Power Meter Sensor	Thorlabs	S121C	1
Photodiode (PD)	Thorlabs	PDA015A2	1
Mirror	CASIX	45°, 99.5% Reflectivity, 660 - 710 nm, Custom Made	4
Collimator	Schäfter + Kirchoff	60FC-F & 60FC (with lenses for 698 nm)	2
AOM	Gooch & Housego	3080-125	1
Faraday Isolator	Excelitas Technologies	FI-680-5SV	1
Polarizing Beam Splitter (PBS)	CASIX	Custom Made (for 660-710 nm)	3
Half Wave Plate (HWP)	Thorlabs	For 698 nm	5
Quarter Wave Plate (QWP)	Thorlabs	For 698 nm	1
Partial Reflecting Mirror (PRM)	Thorlabs	99% Reflection, 1% Transmission, coating for 698 nm	1
Optical Fiber	Thorlabs	SM600 (35 meters)	1
Multimeter	Extech Instruments	Multimeter 420	1
Polarimeter	Schäfter + Kirchoff	SK010PA-VIS	1

7.2. Photos



Figure 8: Mixer

In *Figure 8* the mixer is showed, from above there is a BNC-cable coming down first into the DC-block (BLK-222+), then the BNC-T-splitter and in to the 'L' port of the mixer. Then there is a SMA-cable going into the 'R' port that comes from the LO, and eventually out of the 'I' port first a LPF (BLP-2.5+) and then another BNC-cable that then goes to the PID controller. At the other end of the T-splitter there is another BNC-cable this goes to the Spectrum Analyzer where the measurement is then taken.

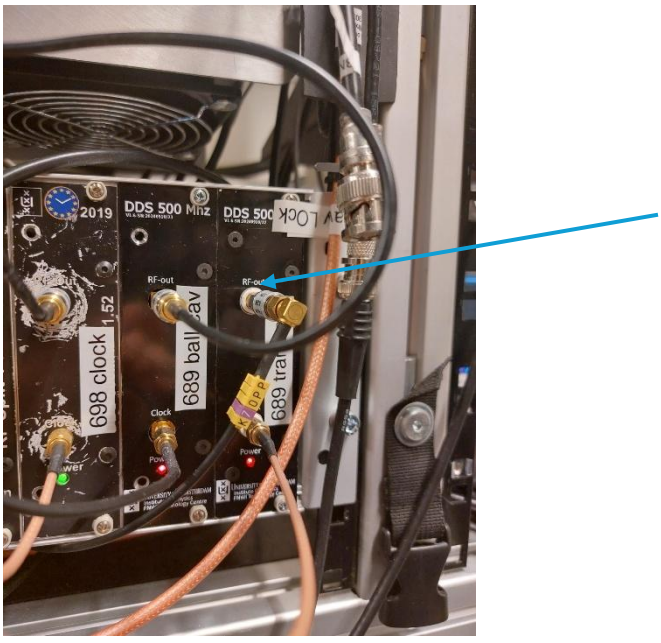


Figure 9: Local Oscillator

In *Figure 9* he local oscillator can be seen (see the blue arrow) that produces the stable 160 MHz RF-signal for mixing with the RF-signal from the photodiode to create the error-signal.

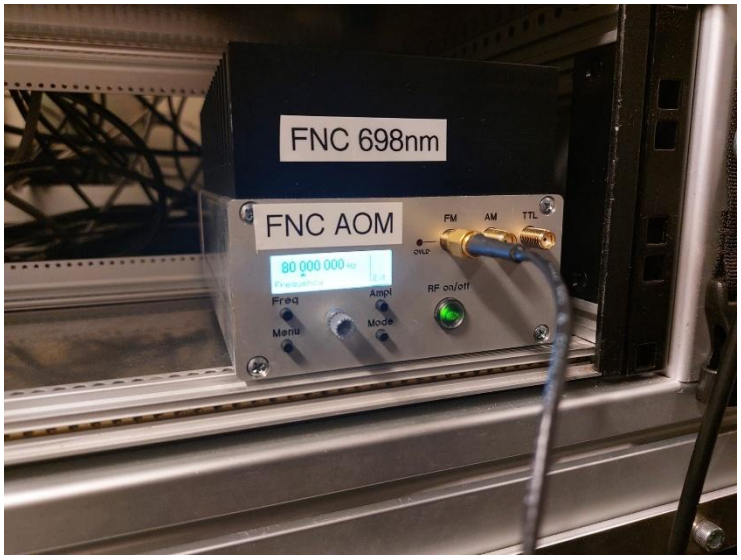


Figure 10: AOM-driver (DDS)

In *Figure 10* the AOM-driver (DDS) is visible with a SMA-cable in the FM port, and the frequency set to 80 MHz.



Figure 11: Red Pitaya

In *Figure 11* the Red Pitaya box is shown, that was used as the digital PID controller for the FNC-system.

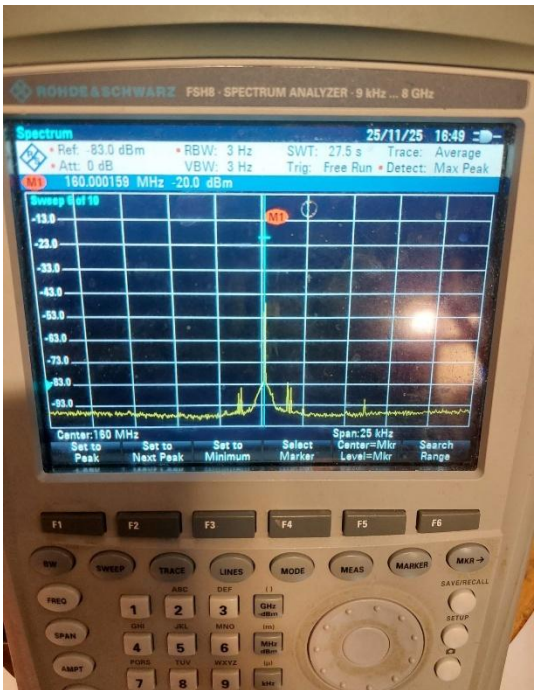


Figure 12: R&S FSH8 Spectrum Analyzer

In *Figure 12* the Spectrum Analyzer is shown that has been used for the measurements. With the Fourier frequency on the x-axis and the power in dBm on the y-axis. The span is set to 25 kHz so the servo-bumps at 42 kHz are not visible here. What is shown here is the spectrum when the FNC-loop is turned on.

0=no Jumper, 1=jumper

MSB				LSB	ERROR GAIN
0	0	0	0	0	5
0	0	0	0	1	10
0	0	0	1	0	15
0	0	0	1	1	20
0	0	1	0	0	25
0	0	1	0	1	30
0	0	1	1	0	35
0	0	1	1	1	40
0	1	0	0	0	45
0	1	0	0	1	50
0	1	0	1	0	55
0	1	0	1	1	60
0	1	1	0	0	65
0	1	1	0	1	70
0	1	1	1	0	75
0	1	1	1	1	80
1	0	0	0	0	85
1	0	0	0	1	90
1	0	0	1	0	95
1	0	0	1	1	100
1	0	1	0	0	105
1	0	1	0	1	110
1	0	1	1	0	115
1	0	1	1	1	120
1	1	0	0	0	125
1	1	0	0	1	130
1	1	0	1	0	135
1	1	0	1	1	140
1	1	1	0	0	145
1	1	1	0	1	150
1	1	1	1	0	155
1	1	1	1	1	160

Table 1: Jumper configuration for setting the Error-gain

In *Table 1* is shown on which pins the jumpers need to be to set a specific error-gain value.

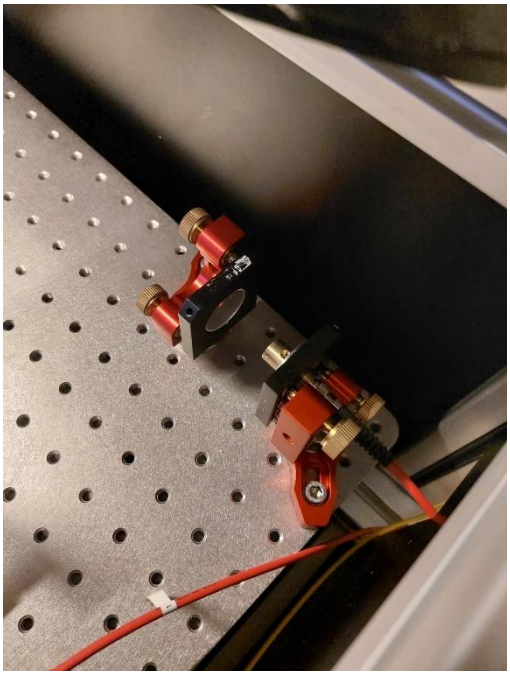


Figure 13: Partially reflecting mirror and collimator

In *Figure 13* the partially reflecting mirror (99/1) and the collimator used for back-reflecting the light to the FNC-setup are being shown.



Figure 14: Laser boxes for the 698 nm laser

In *Figure 14* the two laser boxes that have been used to create the 698 nm ultra-stable laser, including the used settings are visible. The box on the top ‘Fibei Amplifier 1-1064 nm’ was set to 4 A and the Power Stabilization Mode was turned on, the box at the bottom ‘Fibei Amplifier 2-2033 nm’ was set to 13.7 A, these settings for the power of the laser where set following the datasheet of the company ‘Precilasers’.



Figure 15: PyRPL software (FNC-off)

In *Figure 15* the user interface (UI) of the used PyRPL software is visible, this picture shows the error-signal when the FNC-loop is off.

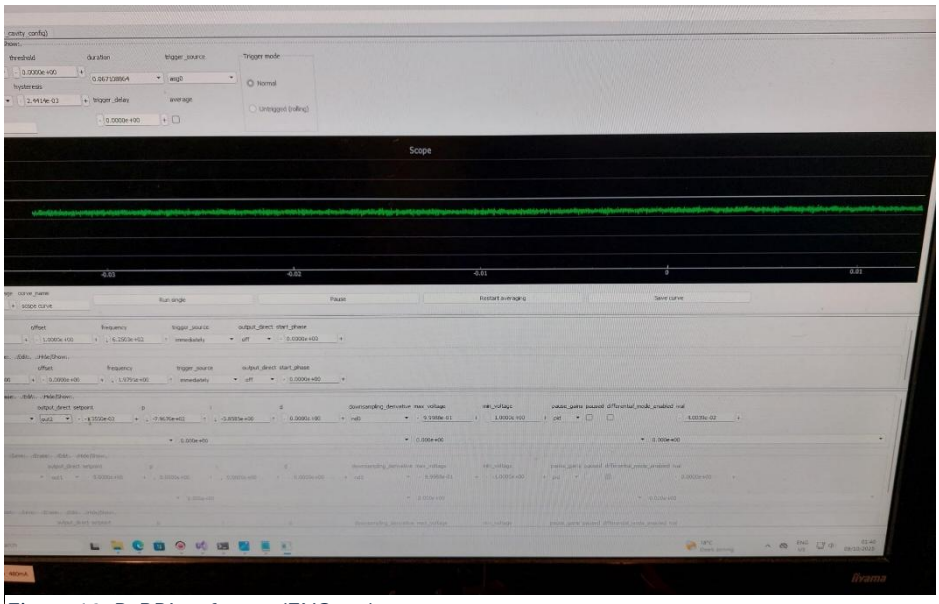


Figure 16: PyRPL software (FNC-on)

In *Figure 16* the same user interface is being shown, only in this case the FNC-loop is on.

7.3. Python code

```
# Analyze function for calculating Frequency noise

def analyze_spectrum(freqs, powers_dBm, RBW, corr_factor):
    # --- 0. Pandas Series -> NumPy arrays ---
    freqs = np.array(freqs)
    powers_dBm = np.array(powers_dBm)

    # --- 1. dBm -> mW ---
    powers_mW = 10**(powers_dBm / 10.0)

    # --- 2. Carrier detection ---
    idx_carrier = np.argmax(powers_mW)
    carrier_freq = freqs[idx_carrier]
    P_carrier = np.sum(powers_mW[idx_carrier-10:idx_carrier+10])

    # --- 3. Calculating Fourier-frequencies ---
    fourier_freqs = freqs - carrier_freq

    # --- 4. Only positive fourier frequencies (one-sided) ---
    mask = fourier_freqs >= 0
    fourier_freqs = fourier_freqs[mask]
    powers_mW = powers_mW[mask]

    # --- 5. Calculating PSD ---
    ENBW = corr_factor * RBW  # Equivalent noise bandwidth
    PSD = powers_mW / ENBW
    L_lin = PSD / P_carrier # 1/Hz
    L = 10 * np.log10(L_lin) #dBc/Hz

    # --- 6. Phase -> frequency noise ---
    S_phi = 2*L_lin  # rad²/Hz
    S_v = fourier_freqs**2 * S_phi

    return S_v, fourier_freqs, L
```